in models and thereby allows detection of cross peaks close to the diagonal. Conversely, the tailings or ridges that result from the phase-twist line shape even under optimal processing conditions can lead to artifacts in the form of apparent cross peaks due simply to the crossing of the ridges from two intense peaks[23,24] (i.e., see apparent cross peaks marked x in Figure 2B). Problems with such apparent cross peaks can be avoided by interpreting only cross peaks whose intensity significantly exceeds that predicted by the sum of the respective ridges. Alternative routes to circumventing the antiphase cancellation of broad peaks are based on the pure absorption cross peaks of the TOCSY experiment.[27,28] However, we find that the substantial pulse power needed to spin-lock over large spectral widths, together with the lengthy mixing times required to develop coherence during which the magnetization of interest decays, severely limits the general utility of this experiment for strongly relaxed lines.[22]

Perhaps the most unique and intriguing prospect for COSY applications in paramagnetic iron tetrapyrrole complexes is the characterization of asymmetric peripheral perturbations on the molecular orbitals of the tetrapyrrole, as reflected in the unpaired spin distribution. Thus the pseudo-4-fold symmetry of a porphyrin can be disrupted via reduction of a pyrrole to yield a chlorin[15,16] (i.e., complex **1**), insertion of a ligand into a pyrrole–iron bond (i.e. carbene insertion[9]), or alkylation of a pyrrole nitrogen[9] (i.e. complexes **3** and **4**). With respect to the N-alkylated ferrous porphyrins, one of the questions that arises is whether the asymmetric spin density reflected in the large spread of the pyrrole (or methylene proton) substituent signals reflects solely asymmetry among the different types of pyrroles or is there large asymmetry even within a pyrrole? Similar questions arise with respect to the large spread of signals in octaethylchlorins.[29] As the data in Figure 4 clearly show for (*N*-methyltetraphenylporphyrinato)-iron(II) (**3**), one pyrrole (likely protons z on the pyrrole trans to the N-alkylated pyrrole of **3**) has large spin density (peak a), one pyrrole (likely protons w on the N-alkylated pyrrole in **3**) has very little spin density (peak c), but the two pyrroles cis to the alkylated pyrrole exhibit a marked asymmetry within that pyrrole ring; one of the protons reflects a large spin density (peak b), while the other one indicates essentially none (peak d). Assignment of the peaks b and d to individual protons x and y in **3** is not yet possible. A slightly different asymmetry is reflected in the $\alpha$-methylene protons of **4**, where the mean $\alpha$-$CH_2$ shift (Table III) is distinctly smaller for only one of the four $\alpha$-$CH_2$ groups (peaks g, h, m). The nature of the delocalized spin density and identity of the molecular orbital(s) in which it resides[1-6] could be determined if the contact shifts of the pyrrole H and $\alpha$-$CH_2$ could be correlated. The present studies clearly show that the first step in the critical assignments needed to elucidate the electronic structure in this class of paramagnetic complexes, as well as others, is readily accessible by modern 2D NMR methods. The next step will be to implement NOESY studies in viscous solvents[14,16] to establish the spatial proximity of noncoupled groups. A search for a viscous solvent chemically compatible with the systems of interest is in progress.

**Acknowledgment.** We thank and are indebted to Drs. M. Renner and C. R. Cornman for experimental assistance. This research was supported by grants from the National Institutes of Health, GM 26226, HL 16087, and HL 22252. The GE NMR Ω-300 and Ω-500 spectrometers were purchased in part with funds from the National Science Foundation, Grants BBS-88-04739 and DIR-90-16484, and the National Institutes of Health, Grant RR-04795.

---

(27) Braunschweiler, L.; Ernst, R. R. *J. Magn. Reson.* **1983**, *53*, 521. Bax, A.; Davies, D. G. *J. Magn. Reson.* **1985**, *65*, 355.

(28) Luchinat, C.; Steuernagel, S.; Turano, P. *Inorg. Chem.* **1990**, *29*, 4351.

(29) Pawlik, M. J.; Miller, P. K.; Sullivan, E. P., Jr.; Levstik, M. A.; Almond, D. A.; Strauss, S. H. *J. Am. Chem. Soc.* **1988**, *110*, 3007.

---

Contribution from the Department of Chemistry, Gorlaeus Laboratories, Leiden University, P.O. Box 9502, 2300 RA Leiden, The Netherlands, and School of Chemical Sciences, Dublin City University, Dublin 9, Ireland

# Mononuclear and Dinuclear Ruthenium Complexes with Triazole-Containing Ligands: Fine-Tuning of the Spectroscopic Properties

Ronald Hage,[†] Jaap G. Haasnoot,[*,†] Jan Reedijk,[†] Renyi Wang,[‡] and Johannes G. Vos[‡]

*Received September 25, 1990*

The synthesis, characterization and properties of mononuclear and dinuclear $Ru(bpy)_2$ complexes with $bpzt^-$ and $mbpt^-$ are reported (bpy = 2,2′-bipyridine, Hbpzt = 3,5-bis(pyrazin-2-yl)-1,2,4-triazole, and Hmbpt = 3-(6-methylpyridin-2-yl)-5-(pyridin-2-yl)-1,2,4-triazole). Both ligands deprotonate easily upon coordination to the $Ru(bpy)_2$ moiety. The coordination mode of the complexes was determined by using $^1H$ NMR spectroscopy. For the mononuclear compounds, $[Ru(bpy)_2(L)]^+$, only coordination via N1 of the triazole ring and the pyridine or pyrazine nitrogen takes place. The two ruthenium centers in the dinuclear compounds with $mbpt^-$ and $bpzt^-$ are bound via N1 and N4 of the triazole ring. Electrochemical and resonance Raman measurements indicate that for $[(Ru(bpy)_2)_2(bpzt)]^{3+}$ and $[Ru(bpy)_2(Hbpzt)]^{2+}$ the first reduction potential is $bpzt^-$ based. $[Ru(bpy)_2(bpzt)]^+$, $[Ru(bpy)_2(mbpt)]^+$, and $[(Ru(bpy)_2)_2(mbpt)]^{3+}$ exhibit a bpy-based reduction. This suggests that in the dinuclear $bpzt^-$ compound and in the protonated compound, the $\pi^*$ level of the $bpzt^-$ ligand is lower than that of the bpy ligand, while the LUMO (lowest unoccupied molecular orbital) is located on the bpy ligand in $[Ru(bpy)_2(bpzt)]^+$. The mixed-valence complexes $[(Ru(bpy)_2)_2(bpzt)]^{4+}$ and $[(Ru(bpy)_2)_2(mbpt)]^{4+}$ exhibit intervalence-transition bands at 5400 $cm^{-1}$ ($\epsilon$ = 2200 $M^{-1}$ $cm^{-1}$) and 5400 $cm^{-1}$ ($\epsilon$ = 2400 $M^{-1}$ $cm^{-1}$), respectively. The extent of electron delocalization is in both cases quite high ($\alpha^2$ = 0.019 and 0.020 respectively), suggesting a fairly strong metal–metal interaction via the HOMO (highest occupied molecular orbital) of the triazolate bridge.

## Introduction

Considerable attention has been paid to dinuclear ruthenium systems, not only because of their potential as two-electron-transfer intermediates in water-splitting devices[1] but also because of the general interest in the physical properties of redox-active dinuclear compounds.[2-16] After partial oxidation of such dinuclear species, mixed-valence species can be obtained, which can yield information about electron delocalization and the degree of metal–metal in-

---

[†] Leiden University.

[‡] Dublin City University.

(1) (a) Seddon, E. A.; Seddon, K. R. *The Chemistry of Ruthenium*; Elsevier Science Publishers BV: Amsterdam, 1984. (b) Meyer, T. J. *Pure Appl. Chem.* **1986**, *58*, 1193. (c) Kalyanasanduram, K.; Grätzel, M.; Pelizzetti, E. *Coord. Chem. Rev.* **1986**, *69*, 57.

(2) (a) Geselowitz, D. A.; Kutner, W.; Meyer, T. J. *Inorg. Chem.* **1986**, *25*, 2015. (b) Gilbert, J. A.; Eggleston, D. S.; Murphy, W. R.; Geselowitz, D. A.; Gersten, S. W.; Hodgson, D. J.; Meyer, T. J. *J. Am. Chem. Soc.* **1985**, *107*, 3855. (c) Vining, W. J.; Meyer, T. J. *Inorg. Chem.* **1986**, *25*, 2023.

0020-1669/91/1330-3263$02.50/0

**Chart I.** Structure and Atomic Numbering of 3,5-Bis(pyridin-2-yl)-1,2,4-triazole (Hbpt), 3,5-Bis(pyrazin-2-yl)-1,2,4-triazole (Hbpzt), and 3-(6-Methylpyridin-2-yl)-5-(pyridin-2-yl)-1,2,4-triazole (Hmbpt)

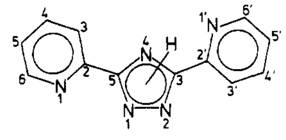

Hbpt

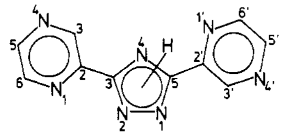

Hbpzt

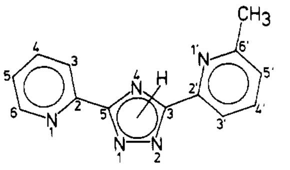

Hmbpt

teraction in these compounds.[11] Recently,[15] we reported the synthesis and properties of mononuclear and dinuclear $Ru(bpy)_2$ compounds (bpy = 2,2′-bipyridine), containing 3,5-bis(pyridin-2-yl)-1,2,4-triazole (Hbpt). The two metal centers in the dinuclear complex are bound via N1 and N4 of the triazole ring (see Chart I). The LUMO (lowest unoccupied molecular orbital) of these complexes are located on the auxiliary bpy ligands as shown by Hage et al.[15] and MacQueen and Petersen.[12c] The two metal-based oxidation potentials of $[(Ru(bpy)_2)_2(bpt)]^{3+}$ differ by about 0.30 V. Electrochemical measurements on isomeric mixed-metal RuOs complexes with $bpt^-$ have revealed that the two coordination sites of the triazole ligand are considerably different.[15b] Also a large amount of electron delocalization has been observed for the $bpt^-$-containing complexes.[15b] It has previously been suggested that hole transfer is a main pathway for the intervalence transfer in mixed-valence species containing anionic bridges.[13b-d] The data obtained for $Ru(bpy)_2$ complexes with bis(benzimidazolate)[16] and bis(pyridyltriazolate)[15b] support this assumption. In order to verify this assumtion, the synthesis and properties of a number of mononuclear and dinuclear "bpt-like" ligands are reported here (see Chart I).

It was anticipated that by changing the structure and by increasing the asymmetry of the ligands, one will be able to obtain more information about the steric and electronic effects that govern the ground-state and excited-state properties of these complexes. The present paper deals with the effect of the level of the LUMO of the bridging ligand on the electrochemical and electronic properties and on the extent of electron delocalization of the mixed-valence species.

## Experimental Section

**Materials.** 3,5-Bis(pyridin-2-yl)-1,2,4-triazole (Hbpt) was prepared as described previously.[15a] 3,5-Bis(pyrazin-2-yl)-1,2,4-triazole (Hbpzt) was prepared as described in the literature for this compound and other substituted triazoles,[17] by using 2-cyanopyrazine[18] as starting material. $^1H$ NMR data ($(CD_3)_2SO$): 9.34 ppm (s, H3), 8.76–8.80 ppm (m, H5 + H6).

3-(6-Methylpyridin-2-yl)-5-(pyridin-2-yl)-1,2,4-triazole (Hmbpt) was synthesized as reported in the literature[17] for similar substituted triazoles by using 2-cyano-6-methylpyridine[18b] as the starting material. $^1H$ NMR data ($(CD_3)_2SO$): 8.67 ppm (d, H6), 8.04 ppm (d, H3), 8.01 ppm (d, H3′), 7.95 ppm (t, H4), 7.82 ppm (t, H4′), 7.44 ppm (t, H5), 7.34 ppm (d, H5′), 2.62 ppm (s, $CH_3$).

The compound *cis*-$[Ru(bpy)_2Cl_2]\cdot 2H_2O$ was prepared according to literature methods from $RuCl_3\cdot xH_2O$ and bpy.[19] $[Ru(bpy)_2(bpt)]PF_6$ and $[(Ru(bpy)_2)_2(bpt)](PF_6)_3$ have been prepared as described previously.[15]

**$[Ru(bpy)_2(bpzt)]PF_6\cdot H_2O$ and $[Ru(bpy)_2(mbpt)]PF_6\cdot CH_3COCH_3$.** $[Ru(bpy)_2Cl_2]\cdot 2H_2O$ (0.5 g; 1 mmol) and 1.2 mmol (0.25 g) of the ligand (Hbpzt or Hmbpt) were refluxed in 50 mL of ethanol/water (2/1) for 6 h. The hot solution was filtered, evaporated until dryness, and dissolved in approximately 10 mL of water. This solution was dropped into an excess of a saturated aqueous $NH_4PF_6$ solution. After filtration, the compound was purified by using column chromatography (neutral alumina; ethanol as eluent). The compound was recrystallized from water/acetone (1/1 v/v).

Anal. Calcd for $[Ru(bpy)_2(bpzt)]PF_6\cdot H_2O$ (**3**): C, 45.00; H, 3.00; N, 19.25; P, 3.88. Found: C, 45.15; H, 2.66; N, 19.05; P, 3.62. Calcd for $[Ru(bpy)_2(mbpt)]PF_6\cdot CH_3COCH_3$ (**5**): C, 50.70; H, 3.76; N, 14.78; P, 3.64. Found: C, 50.68; H, 3.79; N, 14.88; P, 4.04.

**$[(Ru(bpy)_2)_2(bpzt)](PF_6)_3\cdot H_2O$ and $[(Ru(bpy)_2)_2(mbpt)](PF_6)_3$.** The dinuclear compounds were prepared by refluxing 1.2 mmol (0.6 g) of $[Ru(bpy)_2Cl_2]\cdot 2H_2O$ and 1 mmol (0.8 g) of the mononuclear compounds **3** and **5** in 50 mL of water/ethanol for 6 h. Isolation and purification took place as reported for the mononuclear compounds.

Anal. Calcd for $[(Ru(bpy)_2)_2(bpzt)](PF_6)_3\cdot H_2O$ (**4**): C, 39.92; H, 2.66; N, 13.97; P, 5.36. Found: C, 40.04; H, 2.88; N, 13.68; P, 5.36. Calcd for $[(Ru(bpy)_2)_2(mbpt)](PF_6)_3$ (**6**): C, 42.48; H, 2.81; N, 12.16; P, 6.21. Found: C, 42.45; H, 2.82; N, 12.17; P, 6.16.

**Physical Measurements.** UV-vis absorption spectra were recorded on a Perkin-Elmer 330 spectrophotometer using 1-cm quartz cells. The $pK_a$ titrations were carried out on a Shimadzu UV-240 spectrophotometer with matched 1-cm quartz cells by using a Britton–Robinson buffer (a mixture of 0.04 mol $dm^{-3}$ acetic acid, phosphoric acid, and boric acid). Emission spectra were recorded on a Perkin-LS-5 luminescence spectrometer, equipped with a red-sensitive Hamamatsu R928 detector. Emission wavelengths were not corrected for photomultiplier response. The lifetime measurements were performed on an Edinburgh 199 sin-

---

(3) Tinnemans, A. H. A.; Timmer, K.; Reinten, M.; Kraaijkamp, J. G.; Alberts, A. H.; van der Linden, J. G. M.; Schmitz, J. E. J.; Saaman, A. A. *Inorg. Chem.* **1981**, *20*, 3698.

(4) (a) Rillema, D. P.; Callahan, R. W.; Mack, K. B. *Inorg. Chem.* **1982**, *21*, 2589. (b) Rillema, D. P.; Mack, K. B. *Inorg. Chem.* **1982**, *21*, 3849.

(5) Dose, E. V.; Wilson, L. J. *Inorg. Chem.* **1978**, *17*, 2660.

(6) Braunstein, C. H.; Baker, A. D.; Strekas, T. C.; Gafney, H. D. *Inorg. Chem.* **1984**, *23*, 857.

(7) (a) Goldsby, K. A.; Meyer, T. J. *Inorg. Chem.* **1984**, *23*, 3002. (b) Curtis, J. C.; Bernstein, J. S.; Meyer, T. J. *Inorg. Chem.* **1985**, *24*, 385.

(8) Woitellier, S.; Launay, J. P.; Sowinska, M. *Nouv. J. Chim.* **1986**, *10*, 241.

(9) (a) Kober, E. M.; Goldsby, K. A.; Narayana, D. N. S.; Meyer, T. J. *J. Am. Chem. Soc.* **1983**, *105*, 4303. (b) Sullivan, B. P.; Curtis, J. C.; Kober, E. M.; Meyer, T. J. *Nouv. J. Chimie* **1980**, *4*, 643. (c) Sullivan, B. P.; Meyer, T. J. *Inorg. Chem.* **1980**, *19*, 752. (d) Meyer, T. J. *Chem. Phys. Lett.* **1979**, *64*, 417.

(10) (a) Powers, M. J.; Meyer, T. J. *Inorg. Chem.* **1978**, *17*, 1785. (b) Callahan, R. W.; Keene, F. R.; Meyer, T. J.; Salmon, D. J. *J. Am. Chem. Soc.* **1977**, *99*, 1064. (c) Powers, M. J.; Callahan, R. W.; Salmon, D. J.; Meyer, T. J. *Inorg. Chem.* **1976**, *15*, 894.

(11) (a) Hush, N. S. *Prog. Inorg. Chem.* **1967**, *8*, 391. (b) Hush, N. S. *Electrochim. Acta* **1968**, *13*, 1005. (c) Creutz, C. *Prog. Inorg. Chem.* **1983**, *30*, 1.

(12) (a) Wallace, A. W.; Murphy, W. R.; Petersen, J. D. *Inorg. Chim. Acta* **1989**, *166*, 47. (b) Murphy, W. R.; Brewer, K. J.; Getliffe, G.; Petersen, J. D. *Inorg. Chem.* **1989**, *28*, 81. (c) MacQueen, D. B.; Petersen, J. D. *Coord. Chem. Rev.* **1990**, *97*, 249. (d) Cooper, J. B.; MacQueen, D. B.; Petersen, J. D.; Wertz, *Inorg. Chem.* **1990**, *29*, 3701.

(13) Hupp, J. T.; Meyer, T. J. *Inorg. Chem.* **1987**, *26*, 2332.

(14) (a) Rillema, D. P.; Jones, D. S.; Levy, H. A. *J. Chem. Soc., Chem. Commun.* **1979**, 849. (b) Sahai, R.; Baucom, D. A.; Rillema, D. P. *Inorg. Chem.* **1986**, *25*, 3843. (c) Sahai, R.; Morgan, L.; Rillema, D. P. *Inorg. Chem.* **1988**, *27*, 3495.

(15) (a) Hage, R.; Dijkhuis, A. H. J.; Haasnoot, J. G.; Prins, R.; Reedijk, J.; Buchanan, B. E.; Vos, J. G. *Inorg. Chem.* **1988**, *27*, 2185. (b) Hage, R.; Haasnoot, J. G.; Nieuwenhuis, H. A.; Reedijk, J.; De Ridder, D. J. A.; Vos, J. G. *J. Am. Chem. Soc.* **1990**, *112*, 9245.

(16) Haga, M.-A.; Matsumura-Inoue, T.; Yamabe, S. *Inorg. Chem.* **1987**, *26*, 4148.

(17) (a) Browne, E. J.; Ploka, J. B. *J. Chem. Soc. C* **1968**, 824. (b) Browne, E. J.; Ploka, J. B. *J. Chem. Soc.* **1962**, 5149. (c) Kuzmierkiewicz, W.; Foks, H.; Baranowski, H. *Sci. Pharm.* **1985**, *53*, 133.

(18) (a) Delaby, R.; Damiens, R.; Robba, M. *C. R. Seances Acad. Sci., Ser. C* **1968**, *247*, 822. (b) *Organic Synthesis*; John Wiley and Sons: New York, 1973; Vol. 5.

(19) Sullivan, B. P.; Salmon, D. J.; Meyer, T. J. *Inorg. Chem.* **1978**, *17*, 3334.

**Table I.** Relevant $^1H$ NMR Data for the Ruthenium Compounds with 3,5-Bis(pyrazin-2-yl)-1,2,4-triazole (bpzt) and 3-(6-Methylpyridin-2-yl)-5-(pyridin-2-yl)-1,2,4-triazole (mbpt) with Chemical Shifts Listed in ppm Relative to TMS (Measured in $(CD_3)_2CO$)

| | H3 | H4 | H5 | H6 | other |
|---|---|---|---|---|---|
| | | | Mononuclear Compounds $[Ru(bpy)_3(L)]^+$ | | |
| $[Ru(bpy)_2(bpzt)]^+$ | 9.30 + 9.23[a] | | 7.61 + 8.46[a] | 8.36 + 8.46[a] | |
| | 8.70–8.78[c] | 8.02–8.18[c] | 7.46–7.59[c] | 7.88–8.24[c] | |
| $[Ru(bpy)_2(bpzt)]^+$ | 8.26 + 7.93[b] | 8.04 + 7.63[b] | 7.27 + 7.06[b] | 7.73[b] | 2.28 ($CH_3$) |
| | 8.70–8.77[c] | 7.93–8.20[c] | 7.35–7.60[c] | 7.76–8.2[c] | |
| | | | Dinuclear Compounds $[(Ru(bpy)_2)_2(L)]^{3+}$ | | |
| $[(Ru(bpy)_2)_2(bpzt)]^{3+}$ | 9.20 + 7.71[a] | | 7.79 + 7.88[a] | 8.42 + 8.2[a] | |
| | 8.63–8.89[c] | 8.10–8.32[c] | 7.24–7.77[c] | 7.1 + 7.7–8.2[c] | |
| $[(Ru(bpy)_2)_2(mbpt)]^{3+}$ | 6.83 + 8.71[b] | 7.19 + 8.10[b] | 7.18 + 7.21[b] | 7.80[b] | 1.86 + 1.94 ($CH_3$)[b] |
| | 8.67–8.83[c] | 8.06–8.27[c] | 7.3–7.8[c] | 7.61–8.2[c] | |

[a] Resonances of the bpzt⁻ ligand. [b] Resonances of the mbpt⁻ ligand. [c] Resonances of the bpy ligands. [d] Chemical shifts of the methyl peaks of the two geometrical isomers of $[(Ru(bpy)_2)_2(mbpt)]^{3+}$.

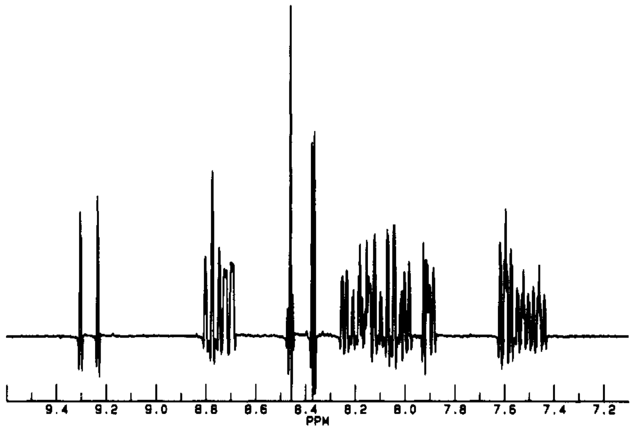

**Figure 1.** Proton NMR spectrum of $[(Ru(bpy)_2)_2(bpzt)]^+$, obtained in $(CD_3)_2CO$ on a 300-MHz spectrometer.

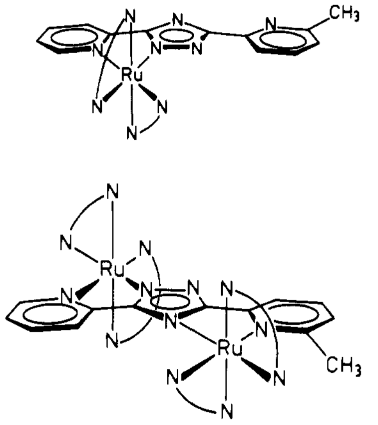

**Figure 2.** Proposed structure of $[(Ru(bpy)_2(mbpt)]^+$ (a, top) and of one geometrical isomer of $[(Ru(bpy)_2)_2(mbpt)]^{3+}$ (b, bottom).

gle-photon-counting instrument. For the room-temperature measurements aerated acetonitrile and at 77 K a mixture of propionitrile/butyronitrile (4:5 v/v) as solvent was used. The single-exponential analysis on the luminescence decay was performed with nonlinear programs,[20] and the quality of the fit was assessed by the $\chi^2$ value close to unity and by a regular distribution of the residuals along the time axis.

Proton NMR spectra of the free ligands were obtained on a Jeol JNM-FX 200-MHz spectrometer with $(CD_3)_2SO$ used as solvent. The complexes were measured in $(CD_3)_2CO$, with TMS as reference. COSY experiments have been performed on a Bruker WM-300 MHz spectrophotometer. Further experimental details of the COSY measurements are given in a previous paper.[15a]

Electrochemical measurements were carried out in a microelectrode cell unit, by using an E. G. and G. Par C Model 303 polarographic analyzer with an E.G. and G. Par 384B universal programmer. A saturated calomel electrode was used as reference electrode. The electrolyte used was acetonitrile containing 0.1 M tetrabutylammonium perchlorate (TBAP). A pulse height of 20 mV for the differential-pulse measurements was used with a scan rate of 4 mV/s. For the cyclic voltammograms the scan rate was 100 mV/s. Electrochemical oxidation was carried out in a homemade three-compartment cell with a platinum sheet as working electrode, a calomel reference electrode, and a platinum wire as auxiliary electrode. A Metrohm E524 coulostat was used to carry out the bulk electrolysis experiments. The spectroelectrochemical experiments were carried out by using an EOT potentiostat in a homemade 1-mm cuvette with a platinum gauze as working electrode, a platinum wire as auxilary electrode, and a quasi-Ag/AgCl wire as reference electrode. Elemental analyses were carried out at University College Dublin.

## Results and Discussion

**Proton NMR Spectroscopy.** As reported previously, NMR spectroscopy is very useful to analyze the structure of the ruthenium(II) compounds.[21-25] The $^1H$ NMR spectra were interpreted by using well-established procedures[21,22] and by comparison with the free ligands. The chemical shifts of the protons of the coordinated substituted triazole ligands have been assigned by using COSY techniques (see Table I and Figure 1).

The X-ray structure and NMR analysis of $[Ru(bpy)_2(bpt)]PF_6$ has revealed that bpt⁻ is coordinated to the ruthenium ion via N1 of the triazole ring.[21f] In the NMR spectrum of $[Ru(bpy)_2(bpzt)]^+$, two different sets of pyrazine rings are present (Table I and Figure 1). The protons of the coordinated pyrazine ring are observed at 9.30 (H3), 7.61 (H5), and 8.36 ppm (H6), while the resonances of the noncoordinated ring are observed at 9.24 (H3) and 8.76 ppm (H5 + H6).

Inspection of the NMR spectrum of $[Ru(bpy)_2(bpzt)]^+$ showed that also in this compound coordination via N1 of the triazole ring takes place. The coordination mode of the ligands can be determined by using NMR spectroscopy, as binding via N4 causes significant steric interaction between the free pyridine/pyrazine ring and an adjacent bulky $Ru(bpy)_2$ group.

---

(20) Bevington, P. R. *Data Reduction and Error Analysis for the Physical Sciences*; McGraw Hill: New York, 1969.

(21) (a) Hage, R.; Prins, R.; Haasnoot, J. G.; Reedijk, J.; Vos, J. G. *J. Chem. Soc., Dalton Trans.* **1987**, 1389. (b) Hage, R.; Haasnoot, J. G.; Reedijk, J.; Vos, J. G. *Inorg. Chim. Acta* **1986**, *118*, 73. (c) Hage, R.; Haasnoot, J. G.; Stufkens, D. J.; Snoeck, T. L.; Vos, J. G.; Reedijk, J. *Inorg. Chem.* **1989**, *28*, 1413. (d) Barigelletti, F.; De Cola, L.; Balzani, V.; Hage, R.; Haasnoot, J. G.; Reedijk, J.; Vos, J. G. *Inorg. Chem.* **1989**, *28*, 1413. (e) Nieuwenhuis, H. N.; Haasnoot, J. G.; Hage, R.; Reedijk, J.; Snoeck, T. L.; Stufkens, D. J.; Vos, J. G. *Inorg. Chem.* **1990**, *30*, 48. (f) Hage, R.; de Graaff, R. A. G.; Haasnoot, J. G.; Turkenburg, J. P.; Reedijk, J.; Vos, J. G. *Acta Crystallogr., Sect. C* **1989**, *C45*, 381. (g) Hage, R. Ph.D. Thesis, Leiden University, 1991.

(22) (a) Lytle, F. E.; Petrosky, L. M.; Carlson, L. R. *Anal. Chim. Acta* **1971**, *57*, 239. (b) Walsh, J. L.; Durham, B. *Inorg. Chem.* **1982**, *21*, 329. (c) Cook, M. J.; Lewis, A. P.; McAuliffe, G. S. G.; Thomson, A. J. *Inorg. Chim. Acta* **1982**, *64*, L25.

(23) (a) Steel, P. J.; Lahousse, F.; Lerner, D.; Marzin, C. *Inorg. Chem.* **1983**, *22*, 1488. (b) Marzin, C.; Budde, F.; Steel, P. J.; Lerner, D. *Nouv. J. Chim.* **1987**, *11*, 33.

(24) (a) Thummel, R. P.; Chirayil, S. *Inorg. Chim. Acta* **1988**, *154*, 77. (b) Thummel, R. P.; Lefoulon, F.; Korp, J. D. *Inorg. Chem.* **1987**, *26*, 2370.

(25) Orellana, G.; Ibarra, C. A.; Santoro, J. *Inorg. Chem.* **1988**, *27*, 1025.

**Table II.** Absorption and Emission Data for the Mononuclear and Dinuclear Complexes

| compd | abs,[a] $\lambda_{max}$, ($\epsilon$) | emission $\lambda_{max}$, nm<br>300 K ($\tau$, ns)[b] | emission $\lambda_{max}$, nm<br>77 K ($\tau$, $\mu$s)[c] | lowest $\pi^*$ |
|---|---|---|---|---|
| $[Ru(bpy)_2(bpt)]^+$ | 475 (0.99) | 678 (70) | 628 (2.8) | bpy |
| $[Ru(bpy)_2(Hbpt)]^{2+}$ | 429 (1.45) | 645 (93) | 610 (3.2) | bpy |
| $[(Ru(bpy)_2)_2(bpt)]^{3+}$ | 452 (2.26) | 648 (56) | 608 (3.6) | bpy |
| $[Ru(bpy)_2(bpzt)]^+$ | 453 (1.42) | 662 (94) | 610 (5.0) | bpy |
| $[Ru(bpy)_2(Hbzt)]^{2+}$ | 441 (1.23) | 670 (118) | 612 (2.6) | bpzt |
| $[(Ru(bpy)_2)_2(bpzt)]^{3+}$ | 449 (2.65) | 670 (106) | 610 (6.4) | bpzt |
| $[Ru(bpy)_2(mbpt)]^+$ | 481 (0.98) | 685 (63) | 628 (2.8) | bpy |
| $[Ru(bpy)_2(Hmbpt)]^{2+}$ | 428 (1.60) | 650 (94) | 610 (3.8) | bpy |
| $[(Ru(bpy)_2)_2(mbpt)]^{3+}$ | 456 (2.02) | 655 (65) | 610 (3.8) | bpy |

[a] Measured in ethanol; values of $\epsilon$ in $10^4$ $M^{-1}$ $cm^{-1}$. [b] Measured in acetonitrile. [c] Measured in propionitrile/butyronitrile (4/5 v/v).

Also for $[Ru(bpy)_2(mbpt)]^+$ two different sets of pyridine protons have been observed (Table I). As expected, the $Ru(bpy)_2$ moiety is bound to the non-methylated pyridine ring. The resonance of the methyl group has shifted 0.34 ppm to higher field, which is caused by the negatively charged triazolate ligand. This coordination mode is expected because now much less steric interaction between the methyl group and an adjacent bpy ligand is present. The structure of this complex is presented in Figure 2a. If the methyl group would be in the vicinity of the bpy ligand, then a much stronger high-field shift would be expected as observed for the $mbpt^-$ dinuclear compound. The NMR data further suggest that the ruthenium ions are also bound via N1 of the triazole ring in $[Ru(bpy)_2(mbpt)]^+$.

The proton NMR spectra of the two dinuclear compounds are very complicated, and no complete assignment could be made. However, by the use of COSY techniques and comparison with the previously reported bis(pyridyl)triazole dimer,[15a] a number of protons of the triazole ligands could be assigned. The two metal ions in this compound are coordinated via N1 and N4 of the triazole ring, as deduced from NMR spectroscopy[15a] and X-ray techniques.[15b] As observed for the dinuclear compound with $bpt^-$, NMR shows the presence of two geometrical isomers with a ratio of about 1:1. Because we have shown previously[15a] that the physical properties of the two geometrical isomers of $[(Ru(bpy)_2)_2(bpt)]^{3+}$ are the same, no attempts have been carried out to separate the two isomers obtained here.

For $[(Ru(bpy)_2)_2(bpzt)]^{3+}$, two sets of pyrazine resonances have been assigned (Table I). H3 of one ring of $[(Ru(bpy)_2)_2(bpzt)]^{3+}$ is observed at 7.71 ppm, and H3 of the other ring of the $bpzt^-$ ligand is located at its normal position (9.20 ppm). This suggests that also in this compound a very short distance between H3 and one of the neighboring bpy ligands is present. This leads to a large shift to higher field of the H3 proton, as previously reported for $[(Ru(bpy)_2)_2(bpt)]^{3+}$.[15a]

In $[(Ru(bpy)_2)_2(mbpt)]^{3+}$, the second ruthenium ion is also bound via N4 to the methyl-containing pyridine ring of $mbpt^-$. The rather short distance between the methyl group and an adjacent bpy ligand causes an upfield shift of this methyl group of 0.7–0.8 ppm. Because of the similarities in NMR data reported here and data for $[(Ru(bpy)_2)_2(bpt)]^{3+}$, the NMR data are not further discussed here.[15a]

The most important conclusion from the NMR data is that in the mononuclear complexes the ruthenium ion is coordinated via N1 of the triazole ring and that in the dinuclear complexes one $Ru(bpy)_2$ group is bound via N1 and the second $Ru(bpy)_2$ moiety is coordinated via N4 of the triazole ring (see Figure 2).

**UV–Vis Absorption Spectroscopy and p$K_a$ Values.** The UV–vis absorption data have been listed in Table II. An intense band has been observed for all complexes in the visible region, which has been assigned to a metal-to-ligand charge-transfer (MLCT) transition.[1]

The acid–base chemistry of $[Ru(bpy)_2(Hbpzt)]^{2+}$ and $[Ru(bpy)_2(Hmbpt)]^{2+}$ has been investigated by using UV–vis absorption titrations (see Experimental Section). In both cases, clear isosbestic points were observed at 318 and 415 nm for $[Ru(bpy)_2(Hmbpt)]^{2+}$ and at 363 and 415 nm for $[Ru(bpy)_2(Hbpzt)]^{2+}$ (Figure 3). The p$K_a$(1) value of $[Ru(bpy)_2(Hmbpt)]^{2+}$ is 4.75 ± 0.1, and the p$K_a$ value of $[Ru(bpy)_2(Hbpzt)]^{2+}$ is 2.0 ± 0.2. The p$K_a$(1) values for the free ligands are 7.1 ± 0.1 for Hbpzt and 8.6 ± 0.1 for Hmbpt. It has previously[15a] been shown for the Hbpt-mononuclear compound, that the p$K_a$(1) value for the free ligand is 8.4 and for the coordinated ligand is 4.0. The change of more than 4 orders of magnitudes has been explained by a net charge flow from the ligand to the metal center. Also for the compounds with $mbpt^-$ and $bpzt^-$, the triazole protons of the coordinated ligands are much more acidic. Removal of the triazole-based proton (p$K_a$(1)) of the coordinated Hbpzt and Hmbpt ligands leads to a red shift of the MLCT bands (see Figure 3). As discussed previously for $[Ru(bpy)_2(Hbpt)]^{2+}$, the $\sigma$-donor properties are stronger for the deprotonated species, yielding a destabilization of the d orbitals.[15a]

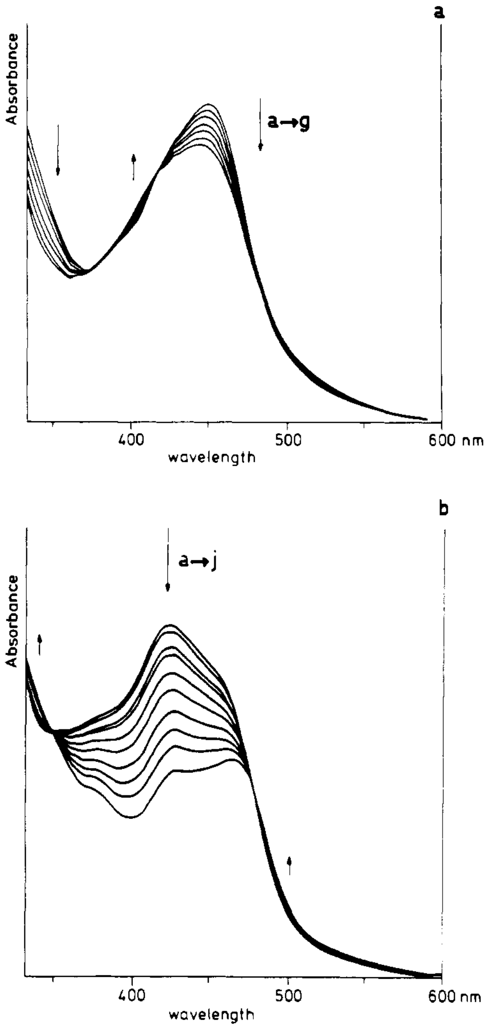

**Figure 3.** (a) Titration of $[Ru(bpy)_2(Hbpzt)]^{2+}$ in a Britton–Robinson buffer with 5 M NaOH. Curves a–g are the measurements at pH 0.56, 1.06, 1.51, 1.90, 2.33, 2.95, and 4.57. (b) Titration of $[Ru(bpy)_2(Hmbpt)]^{2+}$ in a Britton–Robinson buffer with 5 M NaOH. Curves a–j are the measurements at pH 1.95, 2.98, 3.86, 4.07, 4.38, 4.63, 4.91, 5.20, 5.53, and 7.44.

The p$K_a$ value of the free ligand is related to the $\sigma$-donor capacity of the ligand.[26a] The p$K_a$ value for the protonation of bpy is 4.4.[27] Therefore, it can be concluded that, compared to bpy, all deprotonated triazole ligands ($bpt^-$, $mbpt^-$, and $bpzt^-$) have stronger $\sigma$-donor properties.[26b] Compared to free Hbpt and Hmbpt, however, the p$K_a$ value of free Hbpzt is significantly lower,

---

(26) (a) Ernst, S. Ph.D. Thesis, Frankfurt am Main, 1987. (b) Ernst, S.; Kaim, W. *Inorg. Chem.* **1989**, *28*, 1520. (c) Ernst, S.; Kasack, V.; Kaim, W. *Inorg. Chem.* **1988**, *27*, 1146. (d) Kaim, W.; Kasack, V. *Inorg. Chem.* **1990**, *29*, 4696.

(27) Krishnan, C. V.; Creutz, C.; Schwartz, H. A.; Sutin, N. *J. Am. Chem. Soc.* **1983**, *105*, 5617.

**Table III.** Electrochemical Data (V) for the Ruthenium Complexes between +2.0 and −2.0 V vs. SCE with All Differential-Pulse Measurements Carried out in $CH_3CN$ with 0.1 M TBAP

| compound | oxidn potl | | redcn potl | | | | |
|---|---|---|---|---|---|---|---|
| $[Ru(bpy)_2(bpt)]^+$ | 0.85 | | −1.47 | | −1.72 | | |
| $[Ru(bpy)_2(Hbpt)]^{2+}$ | 1.06 | | | | | | |
| $[(Ru(bpy)_2)_2(bpt)]^{3+}$ | 1.04 | 1.34 | −1.40 | | −1.62 | −1.67 | |
| $[Ru(bpy)_2(bpzt)]^+$ | 0.99 | | −1.42 | | −1.62 | −1.96 | |
| $[Ru(bpy)_2(Hbpzt)]^{2+}$ | 1.24 | | | | | | |
| $[(Ru(bpy)_2)_2(bpzt)]^{3+}$ | 1.16 | 1.46 | −1.26 | −1.39 | −1.55 | −1.63 | −1.85 |
| $[Ru(bpy)_2(mbpt)]^+$ | 0.85 | | −1.47 | | −1.72 | | |
| $[Ru(bpy)_2(Hmbpt)]^{2+}$ | 1.06 | | | | | | |
| $[(Ru(bpy)_2)_2(mbpt)]^{3+}$ | 1.04 | 1.34 | −1.37 | | −1.43 | −1.62 | −1.71 |

indicating that the $bpzt^-$ ligand has substantially weaker σ-donor capacity than $bpt^-$ and $mbpt^-$. These conclusions are of importance for the electrochemical measurements and will be discussed in the next section.

Apart from protonation/deprotonation of the triazole ring, also the pyrazine ring can be protonated, as shown previously for $[Ru(bpz)_3]^{2+}$ (bpz = 2,2′-bipyrazine[28]) and for a series of $Ru(bpy)_2(L)$ complexes (L = 3-(pyrazin-2-yl)-1,2,4-triazole)[21e] (eq 1). To determine the $pK_a(2)$ values, titration experiments have

$$[Ru(bpy)_2(bpzt)]^+ \underset{pK_a(1)}{\rightleftharpoons} [Ru(bpy)_2(Hbpzt)]^{2+} \underset{pK_a(2)}{\rightleftharpoons} [Ru(bpy)_2(H_2bpzt)]^{3+} \quad (1)$$

been carried out in concentrated $H_2SO_4$ solutions. Plotting the absorbance vs the acidity strength (Hammett constant[29]) yields a $pK_a(2)$ value of −1.2 for $[Ru(bpy)_2(Hbpzt)]^{2+}$ and a $pK_a(2)$ value of −1.5 for $[(Ru(bpy)_2)_2(Hbpzt)]^{4+}$. No indications for two distinct protonation steps for $[(Ru(bpy)_2)_2(Hbpzt)]^{4+}$ have been found. The $pK_a(2)$ values obtained are very similar to those observed for the $Ru(bpy)_2$ complexes containing pyrazinyltriazole ligands.[21e] No evidence for protonation of the free ring of $[Ru(bpy)_2(Hbpzt)]^{2+}$ has been found in the 300–600-nm region.

**Electrochemical Properties.** As shown in Table III, the oxidation and reduction potentials of the $mbpt^-$-containing complexes are very similar to those of the $bpt^-$ systems.[15a] This is surprising as it was anticipated that the methyl group attached to the pyridine ring would cause an appreciable steric interaction between the bridging ligand and one of the bipyridyl rings.

The metal-based oxidation potentials of bpzt-containing complexes are significantly higher than those observed for the $(m)bpt^-$ analogues. As discussed in the previous section, the bis(pyrazyl)triazole ligand is a weaker σ donor, causing a stabilization of the metal-based orbitals.

The reduction potentials of $[Ru(bpy)_2(mbpt)]^+$, $[Ru(bpy)_2(bpzt)]^+$, and $[(Ru(bpy)_2)_2(mbpt)]^{3+}$ are present at around −1.40 V vs SCE, suggesting a bpy-based reduction in all these systems.[15a,21e] The first reduction potential of $[(Ru(bpy)_2)_2(bpzt)]^{3+}$ is much less negative (Table III), which points to a $bpzt^-$-based reduction process (vide supra). No well-defined reduction waves have been observed for $[Ru(bpy)_2(Hbpzt)]^{2+}$ and $[Ru(bpy)_2(Hmbpt)]^{2+}$, which can be explained by either deprotonation processes upon reduction of the complexes[21a] or by adsorption on the surface of the electrode.[21a,30]

**Resonance Raman Measurements.** In previous studies, it has been shown that resonance Raman (rR) spectroscopy can be used for assignments of MLCT bands of ruthenium(II) systems.[6,31–35]

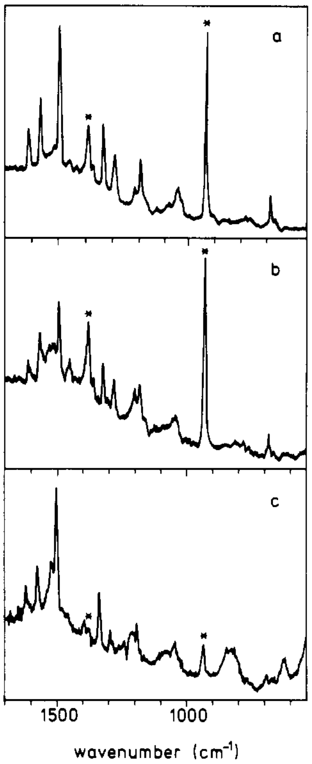

**Figure 4.** Resonance Raman spectra of $[Ru(bpy)_2(bptz)]^+$, excited at 458 nm (a), of $[Ru(bpy)_2(Hbptz)]^{2+}$, excited at 488 nm (b), and of $[(Ru(bpy)_2)_2(bpzt)]^{3+}$, excited at 458 nm (c).

For $[Ru(bpy)_2(bpt)]^+$ and $[(Ru(bpy)_2)_2(bpt)]^{3+}$, the rR spectra showed only enhanced bpy vibrations, and it has been concluded that the lowest energy MLCT absorption band is a $d\pi \rightarrow \pi^*(bpy)$ transition.[21c] From the electrochemical experiments, it has been concluded the lowest π* orbital is located on a bpy ligand for $[Ru(bpy)_2(bptz)]^+$ and most likely on the bridging ligand for $[(Ru(bpy)_2)_2(bpzt)]^{3+}$. No reduction wave could be measured for $[Ru(bpy)_2(Hbptz)]^{2+}$. Resonance Raman measurements on these compounds have been carried out in order to unambigiously determine the nature of the lowest MLCT band.

The rR spectra of $[Ru(bpy)_2(bptz)]^+$ excited at 458, 488, and 514.5 nm are very similar and slow only bpy vibrations at 1613, 1569, 1496, 1324, 1280, 1181, and 1034 $cm^{-1}$ (Figure 4).[33] It can be, therefore, concluded that for this complex the lowest MLCT band is a Ru → bpy transition. The protonated complex exhibits also resonances at 1521, 1455, and 1208 $cm^{-1}$ when excited at 454 or 488 nm (Figure 4). Comparison with the rR data obtained for $[Ru(bpz)_3]^{2+}$ and a series of ruthenium complexes containing 3-(pyrazin-2-yl)-1,2,4-triazole ligands reveals that the latter resonances must be $bpzt^-$ vibrations.[21e,32] The fact that both bpy and $bpzt^-$ vibrations are visible suggests that the protonated mononuclear complex exhibits a Ru → bpy transition as well as a Ru → $bpzt^-$ transition in the MLCT absorption band.

The rR spectrum of $[(Ru(bpy)_2)_2(bpzt)]^{3+}$, excited at 458 nm, exhibits both bpy vibrations and $bpzt^-$ vibrations (Figure 4). The rR spectra obtained at lower energies (488 and 514.5 nm) are too weak to draw firm conclusions from. These data suggest that

---

(28) (a) Rillema, D. P.; Allen, G.; Meyer, T. J.; Conrad, D. *Inorg. Chem.* **1983**, *22*, 1617. (b) Crutchley, R. J.; Kress, N.; Lever, A. B. P. *J. Am. Chem. Soc.* **1983**, *105*, 1170. (c) Crutchley, R. J.; Lever, A. B. P. *J. Am. Chem. Soc.* **1980**, *102*, 7128.

(29) Long, F. A.; Paul, M. A. *Chem. Rev.* **1957**, *57*, 1.

(30) Sullivan, B. P.; Conrad, D.; Meyer, T. J. *Inorg. Chem.* **1985**, *24*, 3640.

(31) (a) Stufkens, D. J.; Snoeck, T. L.; Lever, A. B. P. *Inorg. Chem.* **1988**, *27*, 953. (b) Tait, C. D.; Donohoe, R. J.; DeArmond, M. K.; Wertz, D. W. *Inorg. Chem.* **1986**, *26*, 2754.

(32) Danzer, G. D.; Kincaid, J. R. *J. Phys. Chem.* **1990**, *94*, 3976.

(33) Mabrouk, P. A.; Wrighton, M. S. *Inorg. Chem.* **1986**, *25*, 526.

(34) Kirsch-DeMesmaeker, A.; Jacquet, L.; Masschelein, A.; Vanhecke, F.; Heremans, K. *Inorg. Chem.* **1989**, *28*, 2465.

(35) Fuchs, Y.; Lofters, S.; Dieter, T.; Shi, W.; Morgan, R.; Strekas, T. C.; Gafney, H. D.; Baker, A. D. *J. Am. Chem. Soc.* **1987**, *107*, 2691.

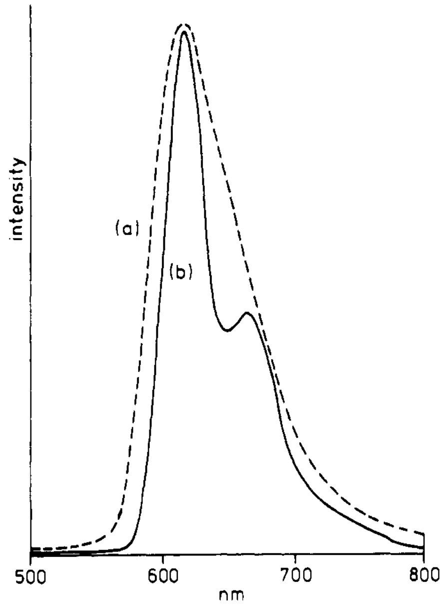

**Figure 5.** Emission spectra of $[(\mathrm{Ru(bpy)_2})_2(\mathrm{mbpt})]^{3+}$ (a) and $[(\mathrm{Ru(bpy)_2})_2(\mathrm{bpzt})]^{3+}$ (b), measured in propionitrile/butyronitrile (4/5) at 77 K.

compared to $[\mathrm{Ru(bpy)_2(bptz)}]^+$, the $\pi^*$ level of the bpzt⁻ ligand in $[(\mathrm{Ru(bpy)_2})_2(\mathrm{bpzt})]^{3+}$ is lowered significantly. This observation is also in agreement with the less negative reduction potential observed for $[(\mathrm{Ru(bpy)_2})_2(\mathrm{bpzt})]^{3+}$.

**Location of the Emitting States.** The emission data in Table II show that apart from the absorption maxima and electrochemical properties the emission properties of the mononuclear and dinuclear complexes containing mbpt⁻ are also very similar to those obtained for the analogous bpt⁻ complexes. It can, therefore, be concluded that the electronic properties of the bis(pyridyl)triazole complexes are not much influenced by the extra methyl group. Previous work on the bpt⁻ systems has unambigiously shown that the emitting states are bpy based.[12c,21d,21g] The similarities between the bpt⁻ and mbpt⁻ systems suggest that in all mbpt⁻-containing complexes, only the auxiliary bpy ligands are directly involved in the emission processes. The electrochemical and rR data show that, for $[\mathrm{Ru(bpy)_2(bpzt)}]^+$, the emitting state is also bpy-based. For $[\mathrm{Ru(bpy)_2(Hbpzt)}]^{2+}$ the situation is different as the rR spectra show both bpy and Hbpzt vibrations. This suggests that, upon protonation of the bpzt⁻ ligand, a significant lowering of the $\pi^*$ (bpzt) orbital takes place. The properties of $[\mathrm{Ru(bpy)_2(bpzt)}]^+$ are very similar to those observed for the pyrazyltriazole-containing complexes, where a switchover from bpy-based emission for the deprotonated complexes to a pyrazyltriazole-based emission for the protonated (and N-methylated) complexes has been observed.[21e] It is likely that the same conclusion can be drawn for the bpzt⁻ complexes.

The $^3$MLCT state of $[(\mathrm{Ru(bpy)_2})_2(\mathrm{bpzt})]^{3+}$ is most likely also bpzt⁻-based, as shown from the electrochemical and rR measurements (less negative reduction potential and more bpzt⁻ character in the rR spectra).[12d] The switchover from bpy-based emission for $[\mathrm{Ru(bpy)_2(bpzt)}]^+$ to a bpzt-based emission for $[(\mathrm{Ru(bpy)_2})_2(\mathrm{bpzt})]^{3+}$ causes nearly identical MLCT energies for these complexes. It has been suggested that upon going from a mononuclear to a dinuclear compound either the empty $\pi^*$ level of the bridging ligand is stabilized and the absorption maximum shifts to lower energy (as found for 2,2′-bipyrimidine[2], 2,3-bis(2-pyridine)pyrazine,[14] or 2,3-bis(2-pyridyl)quinoxaline[14]) or the bridging ligand becomes a weaker $\sigma$ donor so that a blue shift of the MLCT band is observed (as for bis(benzimidazole)[16] and bis(pyridyl)triazoles[15,21d]). When one goes from the mononuclear to the dinuclear compound with bpzt⁻, both effects are observed (Figure 5).

First, a lowering of the $\pi^*$ level of the bridging ligand is observed. Because of the switch from the bpy-based reduction for the mononuclear compound to a bpzt⁻-based reduction for the dinuclear compound, the decrease in energy of the lowest $\pi^*$ level upon the formation of the dinuclear compound is much smaller than observed for other bridging ligands with low-lying $\pi^*$ levels.

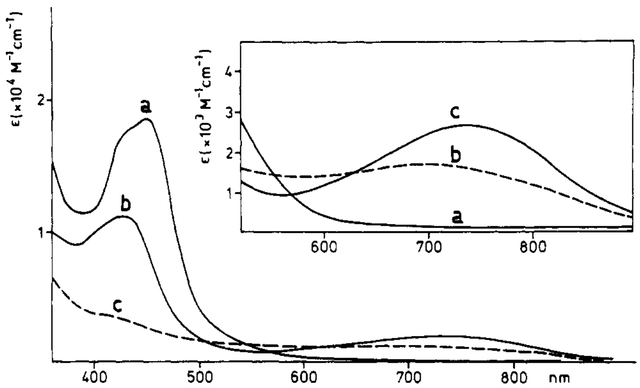

**Figure 6.** Absorption spectra of $[(\mathrm{Ru^{II}(bpy)_2})_2(\mathrm{bpt})]^{3+}$ (a), $[(\mathrm{bpy})_2\mathrm{Ru^{III}(bpt)Ru^{II}(bpy)_2}]^{3+}$ (b), and $[(\mathrm{Ru^{III}(bpy)_2})_2(\mathrm{bpt})]^{3+}$ (c), measured in acetonitrile.

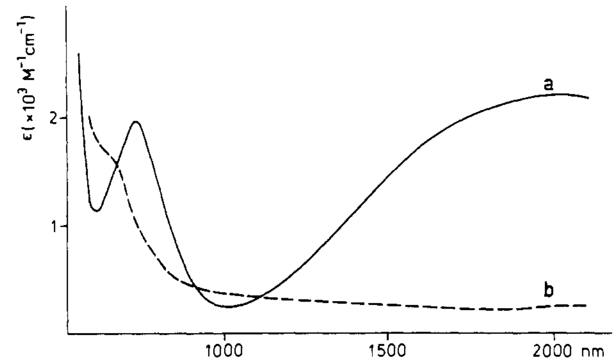

**Figure 7.** Near-infrared spectra of $[(\mathrm{bpy})_2\mathrm{Ru^{III}(mbpt)Ru^{II}(bpy)_2}]^{3+}$ (a) and $[(\mathrm{Ru^{III}(bpy)_2})_2(\mathrm{mbpt})]^{3+}$ (b), measured in acetonitrile.

Second, the higher oxidation potential observed for the bpzt⁻ dinuclear compound compared to the analogous monomer shows that a lowering of the filled d orbital is present. This is caused by the fact that in the dinuclear compound two $\mathrm{Ru(bpy)_2}$ units share the $\sigma$-donor capacity of the negatively charged bridging ligand. As the difference in first reduction potentials for $[\mathrm{Ru(bpy)_2(bpzt)}]^+$ and $[(\mathrm{Ru(bpy)_2})_2(\mathrm{bpzt})]^{3+}$ (0.16 V) is nearly the same as the difference in their oxidation potential (0.17 V). The two effects cancel out and very similar MLCT absorption and emission energies are observed for both compounds. Systems containing bpy-*p*-$\mathrm{CH_2C_6H_4CH_2}$-bpy also exhibit similar absorption/emission energies for the mononuclear and dinuclear complexes, but in this case no or very little interaction between the metal centers is present.[36] As will be shown in the next section, the metal-metal interaction between the two $\mathrm{Ru(bpy)_2}$ moieties is quite strong. Therefore, the switch from a bpy-based to a bpzt-based reduction/emission makes the bpzt⁻ system unique.

**Spectroelectrochemical Measurements.** In order to study the properties of the mixed-valence species and of the fully oxidized complexes, we have performed spectroelectrochemical experiments. The absorption spectra between 900 and 300 nm of $\mathrm{Ru^{II}(bpt)Ru^{II}}$, $\mathrm{Ru^{III}(bpt)Ru^{II}}$, and $\mathrm{Ru^{III}(bpt)Ru^{III}}$ species have been presented in Figure 6. After generation of the mixed-valence species, the band at 452 nm has shifted to 433 nm. Full oxidation leads to disappearance of the band at 433 nm. The same observations have been made for the analogous bpzt⁻ and mbpt⁻ complexes and will therefore not further discussed.

Electrochemical oxidation of $[(\mathrm{Ru(bpy)_2})_2(\mathrm{mbpt})]^{3+}$ to the mixed-valence species, yields two new bands at 770 nm (bandwidth 4000 cm⁻¹) and 1850 nm. Further oxidation to the $\mathrm{Ru^{III}Ru^{III}}$

---

(36) (a) Rye, C. K.; Schmehl, R. H. *J. Phys. Chem.* **1989**, *93*, 7961. (b) Wacholtz, W. F.; Auerbach, R. A.; Schmehl, R. H. *Inorg. Chem.* **1987**, *26*, 2889.

**Table IV.** Properties of the Intervalence Transition of the Mixed-Valence Dinuclear Compounds Measured in $CH_3CN$ ($E_{op}$, $H_{AB}$, and $\Delta\nu_{1/2}$ in $cm^{-1}$; $\epsilon_{max}$ in $M^{-1}\ cm^{-1}$)

| | $E_{op}$ | $\epsilon_{max}$ | $\Delta\nu_{1/2}^{exp}$ | $\Delta\nu_{1/2}^{calc}$ | $\alpha^2$ | $H_{AB}$ |
|---|---|---|---|---|---|---|
| $Ru^{III}(bpt)Ru^{II}$ | 5556 | 2400 | 3300 | 3580[a] | 0.016[b] | 700[c] |
| $Ru^{III}(bpzt)Ru^{II}$ | 5405 | 2200 | 4200 | 3530[a] | 0.019[b] | 740[c] |
| $Ru^{III}(mbpt)Ru^{II}$ | 5405 | 2400 | 4170 | 3530[a] | 0.020[b] | 770[c] |

[a] Calculated by using eq 2. [b] Calculated by using eq 3. [c] Calculated by using eq 4.

species causes a disappearance of the band at 1850 nm and a small shift of the band at 770 nm to higher energy (see Figure 7). The position and bandwidth of the band around 770 nm suggests that this band is due to a ligand-to-metal charge-transfer (LMCT) transition.[15b,16,37,38] The blue shift of the LMCT band upon going from the III–II species to the III–III species is not expected as removal of an electron from the second metal center (with higher oxidation potential) should lead to a red shift of the LMCT band.[39] However, a similar behavior has recently been observed for $[(Ru(NH_3)_5)_2(L^{2-})]^{3+/4+}$ ($L^{2-}$ = 1,4-dicyanamido-2,3,5,6-tetrachlorobenzene dianion),[37] but no explanation for this behavior has been given.

The disappearance of the band at 1850 nm when the complex is fully oxidized shows that this band is an intervalence transition (IT) band. Hush studied the properties of intervalence transitions in mixed-valence species and showed that the band-width at half-height ($\Delta\nu_{1/2}$) can be calculated by using eq 2.[11] $E_{op}$ is the

$$\Delta\nu_{1/2} = [2310(E_{op} - \Delta E)]^{1/2} \tag{2}$$

energy of the intervalence band, and $\Delta E$ is the energy difference induced by the asymmetrical coordination environment (estimated as 800 $cm^{-1}$ from previous work[15b]). The measured and calculated bandwidths agree resonably well, thus further substantiating the assumption that the band at 1850 nm is indeed an IT band. From eq 3, the extent of electron delocalization can be calculated, where

$$\alpha^2 = \frac{(4.2 \times 10^{-4})\epsilon_{max}\Delta\nu_{1/2}}{d^2 E_{op}} \tag{3}$$

$\epsilon_{max}$ = extinction coefficient of the IT band ($M^{-1}\ cm^{-1}$) and $d$ = distance between the metal centers. For a value of $d$ = 6.184 (2) Å, as determined recently by X-ray techniques for the $bpt^-$ dimer,[15b] $\alpha^2$ values have been obtained (Table IV). The degree of electronic coupling between the two metal centers, $H_{AB}$, can be calculated by using eq 4. The three systems investigated show

$$H_{AB} = \left[\frac{(4.2 \times 10^{-4})\epsilon_{max}(\Delta\nu_{1/2})E_{op}}{d^2}\right]^{1/2} \tag{4}$$

very similar properties (Table IV), suggesting that the induced structural and electronic changes of the bridge do not alter significantly the extent of metal–metal communication. For the three triazolate-bridged systems, the extent of electron delocalization is quite large and is in fact comparable with the one found for the $Ru(bpy)_2$ dimer with bis(benzimidazolate).[16] Compared to, for example, $[Ru(bpy)_2(bpm)Os(bpy)_2]^{5+}$ (bpm = 2,2′-bipyrimidine)[7a] ($\alpha^2$ = 0.0024), the complexes containing anionic bridges show a much stronger metal–metal interaction. A possible explanation has been given by Haga,[16] who has shown that the negatively charged bridge induces a greater M(III) $d\pi$–$L\pi$ mixing. After partial oxidation of the complex, the negative charge is partially located on the oxidized center, thus making the bridge less negative. Therefore, the second metal center feels the effect of partial oxidation much more than when no negative charge would be present on the bridging ligand. This also induces the large difference in oxidation potential. These results suggest that the effect of altering the energy of the lowest $\pi^*$ orbital of the bridging ligand has only a small effect on the extent of electron delocalization in the bridged systems. It is therefore likely that the suggestions made by Taube,[13c] Hupp,[13b] and Kaim[26d] that hole-transfer mechanisms are of major importance for systems with negatively charged bridges are valid in our case.

**Concluding Remarks.** The electrochemical, rR, absorption, and emission experiments reveal that the complexes with $bpzt^-$ are very unusual, as $[Ru(bpy)_2(bpzt)]^+$ shows a bpy-based emission/reduction, while $[(Ru(bpy)_2)_2(bpzt)]^{3+}$ exhibits a $bpzt^-$-based emission/reduction. This switchover in location of the LUMO causes minor changes in the absorption and emission MLCT energies in going from mononuclear to dinuclear compounds. Such behavior has only been observed before in systems where the two metal centers are not or very weakly interacting. The $bpzt^-$ and $mbpt^-$ systems do show considerable metal–metal interaction as deduced from the IT bands of the mixed-valence species. The observation that similar absorption and emission energies exist for the mononuclear and dinuclear systems with the $bpzt^-$ ligand is very interesting. Usually, a red-shift is observed in going from the mononuclear to the dinuclear species (due to a significant lowering of the $\pi^*$ orbital) or a blue-shift is present due to the weaker $\sigma$-donor properties of the dinucleating ligand as compared with the mononucleating ligand. The combination of a lowering of the $\pi^*$ level and the weaker $\sigma$-donor capabilities of the bridged $bpzt^-$ ligand causes this unique behavior. The extents of electron delocalization for the three systems reported in this paper are very similar, although the $bpzt^-$ ligand has a lower $\pi^*$ level than the $bpt^-$ or $mbpt^-$ ligands. This suggests that, for the triazolate-containing systems, hole transfer (via the HOMO levels) is the main pathway.

**Acknowledgment.** We thank Johnson Matthey Chemical Ltd. (Reading, U.K.) for their generous loan of $RuCl_3$. We also thank C. Erkelens (Leiden University) for providing the COSY NMR spectra. Furthermore, we thank Prof. V. Balzani, Dr. F. Barigelletti, and Dr. L. De Cola for helpful discussions and for making available the equipment needed for the lifetime experiments. Finally, we are indebted to Mr. T. L. Snoeck and Dr. D. J. Stufkens for the resonance Raman measurements.

---

(37) Aquino, M. A. S.; Bostock, A. E.; Crutchley, R. J. *Inorg. Chem.* **1990**, *29*, 3641.

(38) Haga, M.-A. *Inorg. Chim. Acta* **1980**, *45*, L183.

(39) We thank one the reviewers for pointing out this fact.